Invasion of a sticky random solid: Self-established potential gradient, phase separation, and criticality

S. B. Santra, Santanu Sinha, and Jahir Abbas Ahmed
Department of Physics, Indian Institute of Technology Guwahati, Guwahati-781039, Assam, India
(Received 16 March 2008; revised manuscript received 10 November 2008; published 30 December 2008)

Invasion of a sticky random solid by an aqueous solution is modeled through a chemical reaction. In this reaction, the solid elements dissolve in the solution and redeposit back on the rough interface. A self-established potential gradient (SEPG) in the binding energy of the solid is developed spontaneously and the system gets phase separated into "hard" and "soft" solids. The solution profile is found drifted slowly into the solid by the SEPG with a constant velocity. The system tunes itself to the percolation threshold in the steady state. In the steady state, the system is found consisting of finite clusters of solution molecules followed by a path of redeposited solid as an invasion percolation cluster. A diffusive growth of the interface and the solution inside the solid is found to occur. The nonequilibrium steady state of this dynamical system is found critical and characterized by a power-law distribution of cluster size with an exponent ≈ -2.

DOI: 10.1103/PhysRevE.78.061135 PACS number(s): 64.60.−i, 05.65.+b, 82.45.Bb, 87.10.Rt

I. INTRODUCTION

Fluid invasion and its interface motion in disordered systems have taken a lot of attention in the recent past [1]. For example, fluctuation in fluid invasion [2], crack propagation in solid [3], driven interface in disordered media [4], domain wall propagation in magnets [5], motion of interface in multiphase flow [6], and many others. The interfaces in these examples were characterized by self-affine fractals and their dynamics exhibit critical correlations.

Invasion percolation (IP), a dynamic percolation process, was developed by Wilkinson and Willemsen [7] in order to study the flow of fluid in porous media. In two dimensions (2D), IP was studied with and without trapping. The fractal dimension of the IP cluster with trapping was found as 1.82 [7] which was also verified experimentally [8], whereas the fractal dimension of IP cluster without trapping was found as 1.89 [9] that of the incipient percolation cluster at the percolation threshold p_c. Thus, IP with trapping belongs to different universality class than that of percolation whereas IP without trapping belongs to the same universality class of percolation in 2D [10]. It has been demonstrated recently that the fractal dimension of IP clusters with trapping is nonuniversal and vary with the coordination number of the 2D lattices [11].

A dynamical system is proposed here to study invasion of a semi-infinite sticky random solid (SRS) by an aqueous solution through a chemical reaction. Physically SRS could represent the silica network of, say, borosilicate glasses [12]. Glass is a multicomponent vitreous system. Due to random local chemical environment in such a system, the binding energies of silica with other constituent molecules of the solid are expected to be arbitrary. As the solution invades the solid, the system is found consisting of finite clusters of solution molecules of all possible sizes followed by an invaded path of redeposited solid as an infinite percolation cluster. Existence of finite clusters of invading fluid is absent in IP. During invasion, the system tunes itself to a dissolution threshold $r_c \approx p_c$, the percolation threshold. A self-established potential gradient (SEPG) in the binding energy of the solid is found to develop spontaneously and the system gets phase separated. The solution profile as well as the fluid interface is drifted into the solid at a constant speed. The system evolves to a nonequilibrium steady state characterized by scale free cluster size distribution and thus identified as a self-organized critical (SOC) state [13]. These are new observations in the context of chemical kinetics of invasion of a complex system.

II. MODEL

In order to study the time evolution of such a SRS in contact with an aqueous solution, a numerical model of a chemical reaction is developed in 2D. The SRS shown in Fig. 1(a) is a dense structure of elements with random binding energy r_i represented on a semi-infinite square lattice. The random binding energy is assumed to be uniformly distributed between 0 and 1. The solid is of width L along y direction and infinitely long in the x direction. A constant source of aqueous solution is kept at the left end of the solid. The solution is represented by white space in Fig. 1. The thick line represents the interface between the solid and the solution. The most weakly bound element R of the SRS on the interface dissolves in the solution S and makes a complex RS. The solution invades into the place of the dissolved solid. The compound RS in the solution breaks almost instantaneously into R and S. The solid element R in the solution is now available for redeposition on the modified rough interface. Because of redeposition of the solid, the solid is rebuilt and it is called sticky. The chemical reaction of dissolution-redeposition can be represented as

$$R + S \rightarrow RS \rightarrow R + S. \tag{1}$$

Assuming diffusion of the solid element R in the solution is very fast, redeposition is made with unit probability at a randomly chosen site on the rough interface accessible to the solution. Generally, dissolution is a slower process than redeposition and it is mimicked here by considering no further dissolution during redeposition. The dynamics of the system

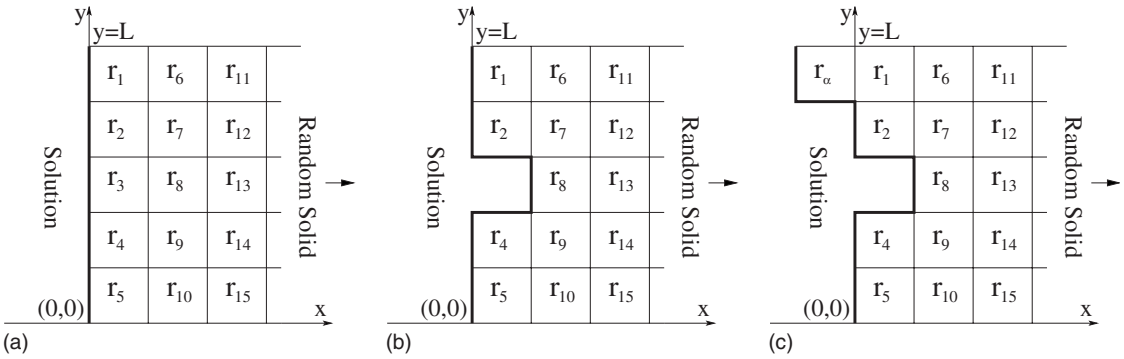

FIG. 1. A single MC step is represented here. (a) The arrangement of random numbers r_i represents the SRS of width $L=5$, (b) r_3 is identified as minimum random number on the interface and it is dissolved, (c) the solid element is redeposited at a randomly chosen site r_1 of the modified interface. A new random number r_α is assigned with the redeposited site. The process is repeated. The arrows on the right-hand side indicate the extension of the solid in that direction.

then involves dissolution and redeposition processes together with reconstruction of the rough interface at the single particle level. The process is very similar to that of glass dissolution in aqueous solutions [14]. Different numerical processes involved in a single Monte Carlo (MC) step are explained with the help of Fig. 1. The processes are (i) extraction of externally accessible perimeter of the solid, (ii) dissolution of the site with minimum random number (minimum binding energy) on the perimeter with unit probability [it is r_3 in Fig. 1(b)], (iii) modification of the external perimeter, (iv) redeposition of the solid element present in the solution on a randomly chosen site of the modified interface [r_1 in Fig. 1(c)], (v) assignment of a new random number r_α to the redeposited site. The whole process is then repeated and time is increased from t to $t+1$. Periodic boundary condition is applied in the y direction. The system then evolves at equal solid to liquid and liquid to solid flux rate (one particle per time step) throughout the simulation.

In Fig. 2, time evolution of the system morphology is shown for $L=64$. The solution is represented by white and the solid is represented by gray. The interface is represented by black. The redeposited solid is shown by intermediate gray. It can be seen that the solution molecules have penetrated into the solid, they form clusters and move collectively. The solution clusters are seem to be pushed into the solid by the redeposited solid elements. The redeposited solid forms an infinite percolation cluster or an IP cluster. In usual IP, an invasion cluster is formed by the invading fluid itself whereas here it is formed by the redeposited solid elements. Thus, at any instant of time the system is composed of finite solution clusters and an infinite percolation (or IP) cluster of redeposited solid. It is important to note that the solid element that dissolves in the lakes of solution inside the solid is also available for redeposition anywhere on the interface. The solution inside the solid is assumed to be connected to the solution sea [15]. During invasion, the solution inside the solid leaves behind a restructured solid. It can be seen that all the solid elements in the restructured part are not replaced by a new random element. The redeposited solid, represented by intermediate gray, indicates the percolating path of the solution molecules. The solid has also grown in the negative x direction almost without holes. The formation of restructured solid is a common phenomenon in glass alteration experiments where a dry silica gel forms on the interface [14].

Simulations have been performed on the square lattice of widths ranging from $L=64$ to 1024 in multiple of 2. Data are averaged over $\mathcal{N}=10^3$ to 10^4 ensembles.

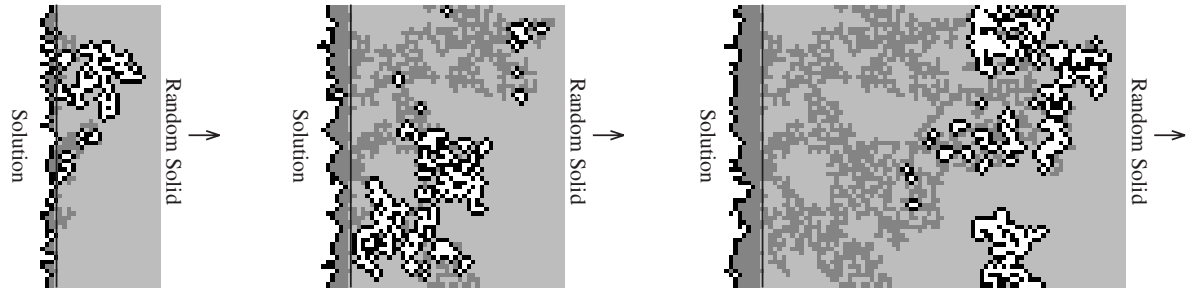

FIG. 2. Morphology of the SRS of width $L=64$ at time steps (a) $t=2^9$, (b) $t=2^{11}$, and (c) $t=2^{12}$. The solution is represented by white, gray represents the solid, black represents the interface, and the redeposited solid is represented by intermediate gray. The vertical solid line represents the initial interface.

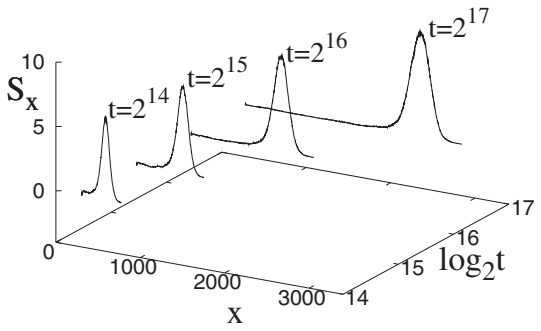

FIG. 3. Solution profile S_x, number of solution molecules per column, as a function of the column index x, is shown at different time t for a system of width $L=64$.

III. SOLUTION PROFILE

In order to characterize the motion of the solution molecules inside the solid, the profile of the solution molecules is determined as a function of the penetration depth along x. The solution profile is defined as the average number of solution molecules S_x in a column x. In Fig. 3, S_x is plotted against x at different time t for $L=64$. It can be seen that the solution molecules move inside the solid as a Gaussian profile leaving behind a restructured solid. The dynamics of the solution profile could be monitored by noting the peak position x_p and the width σ of the profile with time t. The average peak position x_p of a profile is defined as

$$x_p(t) = \frac{1}{\mathcal{N}} \sum_{j=1}^{\mathcal{N}} x_j(S_{\max}), \tag{2}$$

where x_j is the coordinate of the column with maximum number of solution molecules $S_{\max}$ at time t in an ensemble and $\mathcal{N}$ is the number of ensembles. The width σ_j of the solution profile of a given ensemble is defined as

$$\sigma_j = \left(\frac{1}{x_{\max}} \sum_{i=0}^{x_{\max}} (x_i - x_p)^2 \right)^{1/2}, \tag{3}$$

where x_i is the coordinate of a column with a nonzero number of solution molecules S at time t. The average width σ of the profiles is obtained by taking ensemble average, $\sigma = \Sigma_{j=1}^{\mathcal{N}} \sigma_j / \mathcal{N}$. The peak position x_p and the width σ are plotted against time t in Figs. 4(a) and 4(b), respectively. Both x_p and σ increase as power laws with time t. The peak position moves forward linearly $x_p \sim t$ whereas the width increases as $\sigma \sim t^{2/5}$ with time t. The change in x_p is due to dissolution of solid elements in the front whereas σ increases due to the motion of the front but it decreases due to the redeposition of the solid elements. The solution profile thus has a drifted motion inside the solid. Backward motion of the solution profile is less probable because the unexplored solid in the front is always expected to contain a site with lower binding energy. It can be noticed that data for systems of different linear dimensions L collapses onto a single curve after time rescaling $t' = t/L$ as shown in the inset of Fig. 4(a). Thus, time t is proportional to the linear dimension L of the system in this problem. The solution profile then penetrates the SRS at a constant drift velocity proportional to $1/L$. It is thus a slow moving front for large L. The system then achieves a nonequilibrium steady state. It should be mentioned here that in the study of dissolution of a finite random solid in an infinite solution, the steady state was found to achieve a dynamical equilibrium and it was characterized as a self-organized critical state [16].

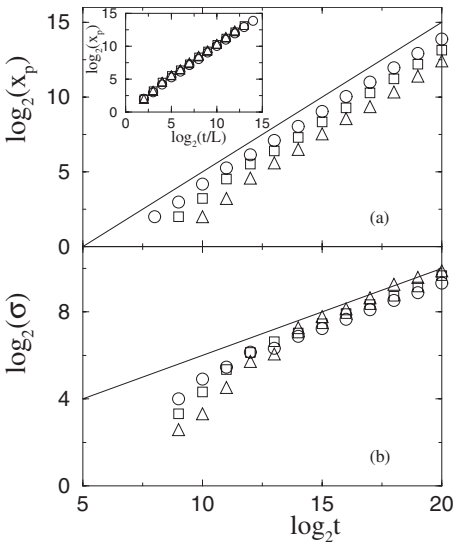

FIG. 4. Plot of (a) the profile peak position x_p and (b) the width σ against time t. It is found that x_p increases linearly with time as $x_p \sim t$. The data collapses onto a single curve with time rescaling $t' = t/L$ as shown in the inset of (a). The profile width increases as $\sigma \sim t^{2/5}$. Different symbols correspond to systems of different width L: (○) for $L=64$, (□) for $L=128$, (△) for $L=256$.

IV. DISSOLUTION THRESHOLD

The distribution of binding energies of the solid elements on the interface at the steady state is calculated to determine the dissolution threshold. The probability to find a solid element of binding energy r on the interface is given by

$$P_I(r,t) = n_r(t)/I, \tag{4}$$

where $n_r(t)$ is the number of elements with binding energy r and I is the length of the interface at time t. The distribution $P_I(r,t)$ is plotted in Fig. 5. It can be seen that the initial uniform distribution (solid line) is spontaneously evolved to a steplike distribution. It is expected that the final distribution would be a θ function around $r_c = p_c$, the percolation threshold (≈ 0.59), as

$$P_I(r,t) = \frac{P_I(r,0)}{(1-p_c)} \theta(r - p_c), \tag{5}$$

where $P_I(r,0) = 0.1$. The θ function is shown by a dashed line. The dissolution will then occur for the energy range $\leqslant r_c$. This is expected because at each dissolution the solution comes in contact with a new solid element with a binding energy between 0 and 1. It is interesting to note that, the system organizes itself to a dissolution threshold around p_c in the steady state though there is redeposition and the front is still able to find the infinite percolation cluster. In the case of

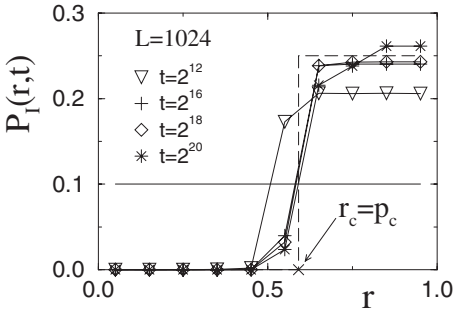

FIG. 5. Probability distribution $P_I(r)$ of the random binding energy of the solid elements on the interface at different times. The solid line represents the initial distribution and the dashed line represents the θ function around $r_c \approx 0.59$.

IP, the system is also tuned to p_c [17] however the system does not include the process of redeposition. It should be emphasized here that the dynamics observed here is independent of the distribution of initial binding energy. For example, SRS with random numbers uniformly distributed between 0.5 to 1 will not lead to a different dynamics.

The dynamical process of dissolution and redeposition considered here is different from dynamical percolation developed by de Freitas *et al.* [18]. In their model, the site occupation probability p increases linearly with time and swept past through p_c whereas in the present model the system tunes itself spontaneously to p_c. Recently, percolation problem is also demonstrated as a self-organizing system by Grassberger and Zhang [19] and Alencer *et al.* [20] in two different models. Grassberger and Zhang [19] reformulated the percolation problem as a time-dependent problem and studied at several values of p in a single run. p_c emerges as a singularity in the time-dependent distribution. Alencer *et al.* [20] studied growth mechanism of percolation clusters by controlling the number of sites in the growth front and the system spontaneously reaches to a stationary state corresponding to p_c. The dynamical rules considered in these self-organizing models are different from that considered in the present model.

V. REDEPOSITED SOLID

The path constituted by the redeposited solid is extracted here. A part of the redeposited path generated on a sample of width $L=256$ over a horizontal extension 512 is shown in Fig. 6. It can be seen that it is a connected path and the cluster of the redeposited solid elements is rarefied and has holes (unexplored solid) of all possible sizes as in an infinite percolation cluster. Note that, an IP cluster is formed by the invading fluid whereas here it is formed by the redeposited solid. Moreover, there is a basic difference between the redeposited solid and the infinite percolation cluster. All the sites of an infinite percolation cluster are occupied with equal probability $p=p_c$. However, redeposition is made here with unit probability at a randomly chosen site and a random number (between 0 and 1) has been assigned to it. In contrary, no random number is associated with the sites of an IP cluster. In the long term evolution, most of the sites of the

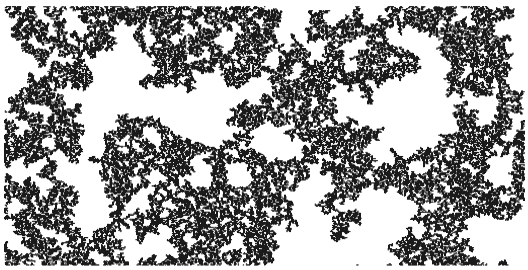

FIG. 6. A part of the path of the redeposited solid in a sample of width $L=256$ and horizontal extension 512. There is periodic boundary condition along the y direction.

redeposited solid has a random number $r > p_c$ associated with it. The system swept past through p_c as in the case of dynamical percolation developed by de Freitas *et al.* [18]. Usually the IP clusters are characterized by its fractal dimension. In order to characterize the redeposited path, its fractal as well as chemical dimensions are measured and the scaling relation among them has been verified below.

Fractal dimension d_f of the redeposited path is estimated on a lattice of width $L=256$ and $L=512$. As the system achieves the steady state (after sufficiently long time), an intermediate portion of dimension $L \times L$ of the solid is taken and box counting method has been applied to calculate d_f of the redeposited path. Note that the solid considered does not contain any solution molecule. In the box counting method, the number of boxes $N_B(\epsilon)$ with at least one redeposited site is expected to scale with the box size ϵ as

$$N_B(\epsilon) \sim \epsilon^{-d_f}. \tag{6}$$

Data are averaged over different samples as well as placing the $L \times L$ box at different places in the intermediate region of the solid of a given sample. $N_B(\epsilon)$ is plotted against ϵ in Fig. 7 for $L=256$ (circles) and $L=512$ (squares). From the slope, it is found $d_f = 1.88 \pm 0.01$. Data for different L is scaled by L^{d_f} assuming $d_f = 1.88$. A good collapse is observed. The mass $M(\epsilon)$ in a given box size ϵ then varies as

$$M(\epsilon) \sim \epsilon^{d_f}. \tag{7}$$

Thus d_f obtained from box counting is consistent with Eq. (7) as expected. The value of the fractal dimension obtained

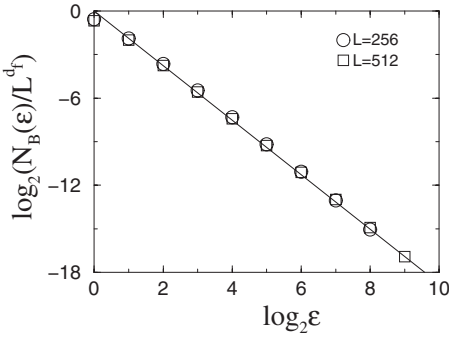

FIG. 7. Plot of the number of boxes $N_B(\epsilon)$ against the box size ϵ for $L=256$ (○) and 512 (□). From the slopes, the fractal dimension d_f is obtained as 1.88 ± 0.01. The data are scaled with L^{d_f} and a good collapse is found.

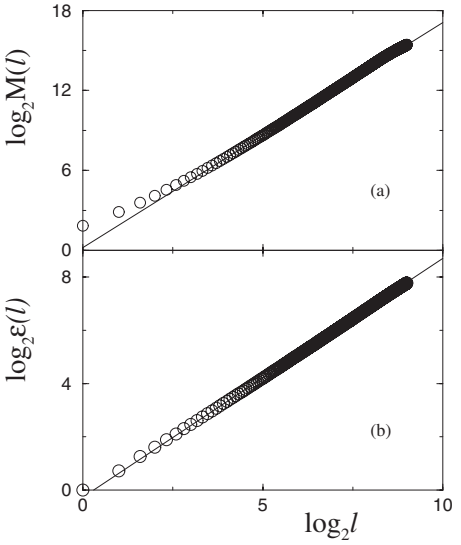

FIG. 8. Plot of (a) average mass $M(\ell)$ and (b) euclidean distance $\epsilon(\ell)$ versus chemical distance ℓ for $L=512$. From (a), the chemical dimension d_ℓ of the redeposited solid is obtained as 1.69 ± 0.02. The exponent $\bar{\nu}$ is obtained from (b) as 0.89 ± 0.01.

here is close to d_f of the infinite percolation cluster (91/48) [21] as well as that of the IP cluster without trapping (1.89) [9]. In IP with trapping, the invader can no longer enter into a region once surrounded by it and the fractal dimension was found as 1.82 [11]. This is not the situation here. Though there are regions of unexplored solid surrounded by hard boundary of redeposited elements, the solid element on the boundary with the lowest energy will always dissolve and the situation corresponds to IP without trapping. Note that, in IP without trapping the front remains connected, however, it is disconnected here.

The fractal dimension only describes the geometric structure of a fractal object which is not sufficient to characterize its structural properties fully. It is essential to characterize the topological structure by the chemical dimension d_ℓ which can be used to distinguish different fractal structures with similar fractal dimension [21]. The chemical dimension d_ℓ is defined as

$$M(\ell) \sim \ell^{d_\ell}, \tag{8}$$

where $M(\ell)$ is mass of the structure within a chemical length ℓ. The chemical distance between two sites of a cluster is defined as the length of the shortest connecting path between them. The chemical distance of the redeposited solid is determined following Ref. [22]. A site on the redeposited solid is chosen randomly as origin. The redeposited nearest-neighbor elements of this site define a shell of chemical distance 1 from the origin. Similarly, the redeposited next nearest neighbors of the origin form a shell of chemical distance 2 and so on. The number of occupied sites within a shell of chemical distance ℓ is counted to measure $M(\ell)$. In Fig. 8(a), $M(\ell)$ is plotted against ℓ for $L=512$. The 500 samples are considered at $t=2^{20}$. On each sample, 5000 different redeposited sites are chosen randomly as origin and data is averaged over them. From the slope, the chemical dimension is obtained as $d_\ell=1.69\pm0.02$. This is close to the chemical dimension ($d_\ell=1.678\pm0.005$) of the incipient percolation cluster at $p=p_c$ in 2D [23].

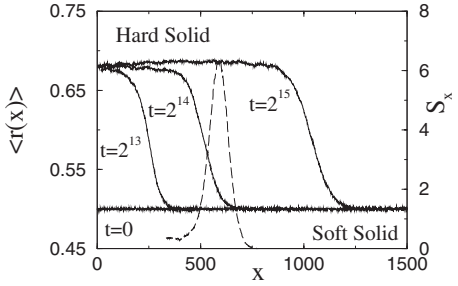

FIG. 9. Plot of average energy $\langle r(x)\rangle$ versus x for $t=2^{13}$, 2^{14}, and 2^{15} for $L=64$. Initial value of $\langle r(x)\rangle=0.5$ is plotted at the bottom. Solution profile S_x at $t=2^{14}$ is also plotted and shown by a dashed line.

A relation between the chemical distance ℓ between two sites and the Euclidean distance ϵ between them can be obtained as

$$\epsilon(\ell) \sim \ell^{d_\ell/d_f} = \ell^{\bar{\nu}} \tag{9}$$

following Eqs. (7) and (8). Measuring ϵ as a function of ℓ, it is possible to determine the exponent $\bar{\nu}$ directly and verify the scaling relation $\bar{\nu}=d_\ell/d_f$. In Fig. 8(b), $\epsilon(\ell)$ is plotted as a function of ℓ. From the slope, the exponent $\bar{\nu}$ is obtained as 0.89 ± 0.01. Here, $d_\ell/d_f=0.90\pm0.03$ and thus the scaling relation $\bar{\nu}=d_\ell/d_f$ is satisfied within error bar. The fractal as well as topological dimensions of the redeposited path is thus similar to that of percolation cluster or IP cluster without trapping. The redeposited path then belongs to the same universality class of percolation or IP without trapping.

VI. SEPG AND PHASE SEPARATION

The solution profile is found drifted slowly into the solid though there is no direct force applied to the solution profile. Initial difference in the chemical potentials $\Delta\mu$ between the solution and the solid at the interface could be the only source of a potential gradient in this system. Since the volume of the solution is assumed to be infinitely large, $\Delta\mu$ is expected to be constant throughout the simulation. The chemical reaction considered here converts $\Delta\mu$ spontaneously into a potential gradient in the average energy of the SRS. The driving force to the solution profile appears from this self-established potential gradient in the binding energy of the solid. Consequently, the solid is phase separated into a restructured "hard" solid and the uninvaded original "soft" solid. To distinguish the restructured "hard" solid from the original "soft" solid, the average energy $\langle r(x)\rangle$ of a column of index x has been calculated as a function of x. In Fig. 9, $\langle r(x)\rangle$ is plotted against x for $t=2^{13}$, 2^{14}, and 2^{15}. The initial average energy of the unexplored solid should be

$$\langle r(x)\rangle_{\text{soft}} = \int_0^1 rP_0(r)dr, \tag{10}$$

where $P_0(r)$ is the initial distribution of random numbers in the solid. Since it is uniformly distributed between 0 and 1,

$\langle r(x)\rangle_{\text{soft}}=0.5$ and it is shown at the bottom in Fig. 9. The average energy of the hard solid is expected to be

$$\langle r(x)\rangle_{\text{hard}} = \int_0^1 rP'(r)dr, \tag{11}$$

where $P'(r)$ is the distribution of binding energies of the invaded solid which includes redeposited solid as well as the unexplored solid (see Fig. 6) and thus the limit should extend from 0 to 1. However, the distribution energy of the redeposited solid is expected to be uniform in the range p_c to 1 at $t\to\infty$ limit (see Fig. 5). It can be seen that the average energy of the hard solid is found to be lower than 0.7. It is found that the solution profile at a given time is situated just in front of the potential gradient developed at that time (see Fig. 9 for $t=2^{14}$). The SEPG is thus pushing the solution profile deep into the solid and responsible for the drifted motion of the solution profile. It is important to note that the gradient in the average energy has developed spontaneously and leads to phase separation in the system into "hard" and "soft" solids. Spontaneous phase separation by a self-established potential gradient in the invasion of complex solid is a new observation. This was not observed in the earlier models of glass dissolution studies [15,24] may be due to rapid dynamics considered there. Since redeposition is absent in IP, $\langle r(x)\rangle$ will have higher value in the uninvaded part in comparison to the invaded part in contrast to the present situation.

The development of the potential profile and its motion inside the solid is very similar to front propagation in reaction diffusion systems [25] and biological pattern formation [26]. In these cases, a steady-state solution of one-dimensional (1D) Fisher-Kolmogorov (FK) equation [27] corresponds to an interface moving with a constant velocity as observed here. A steady-state solution to 1D FK equation for a field ϕ is also obtained here for an interface between $\phi=1/2$ and $4/5$. However, the solution to 1D FK equation here is found to be highly sensitive to the initial conditions.

VII. CLUSTER DYNAMICS

As the potential profile pushes the solution molecules deep inside the solid, they form clusters and move collectively. It is a process of self-clustering inside the valleys of the dynamically evolved potential distribution defined by the random numbers assigned to the lattice sites initially as well as to the redeposited sites. Note that these are not exactly the percolation clusters in which the sites are occupied with a prefixed probability p. In that sense, the clusters are like IP clusters. However, the clusters here are disconnected and finite unlike IP. This self-clustering of solution molecules is similar to the case of clustering of passive sliders on stochastically evolving surfaces [28]. The length of the interface and the volume of the solution inside the solid grow with time. It is important to check the nature of the growth of the solid-liquid interface as well as the volume of the solution inside the solid. These two growth processes are studied by noting the number of solid elements I on the interface and the number of solution molecules S inside the solid as a function of time t. I and S are plotted in Figs. 10(a) and 10(b), respectively, against the rescaled time $t'=t/L$. Note that I as well as S also scale with the system size L. It is found that both I and S are growing with time as

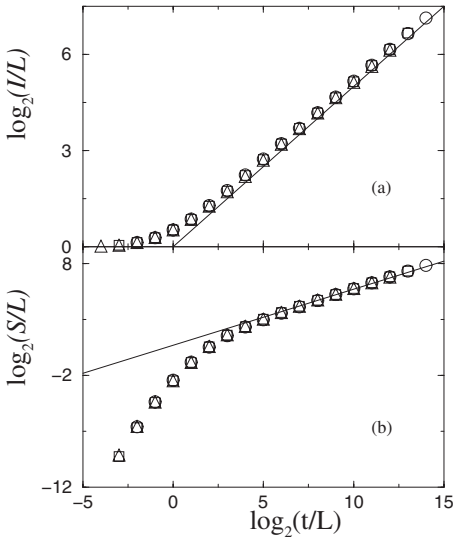

FIG. 10. Plot of (a) the solid interface elements I and (b) the solution molecules S inside the solid against the rescaled time $t'=t/L$. Different symbols correspond to systems of different width L: (○) for $L=256$, (□) for $L=512$, (△) for $L=1024$. I and S both also scale with the system size L. From the slopes, both I and S are found to grow with time as $I\sim\sqrt{t'}$ and $S\sim\sqrt{t'}$ in the long time regime.

$$I\sim\sqrt{t'} \quad \text{and } S\sim\sqrt{t'} \tag{12}$$

in the long time regime. The interface as well as the volume of the solution then have a diffusive growth when the solution profile is drifted inside the solid at a constant velocity by the SEPG.

The interface evolution in the present model has great similarity with the Bak-Snappen (BS) model of biological evolution [29]. In the BS model, time evolution of the fitness string of a number of species was considered. The fitness of a species was represented by a random number uniformly distributed between 0 and 1. The species with the lowest fitness (lowest random number) was replaced by another random number and the fitness string was locally modified as the interface is modified locally here in the present model. The BS model self-organizes into a critical state with intermittent coevolutionary avalanches of all sizes representing punctuated equilibrium behavior of the evolution process. The fitness string in the BS model never had a hole, always a single continuous string, unlike the interface here which could be a collection of external perimeters of all finite disconnected clusters.

VIII. CRITICALITY

In order to verify the criticality of the system, the dynamical cluster size distribution of the finite clusters formed by solution molecules are determined. The probability to have an s-sited cluster at time t is given by

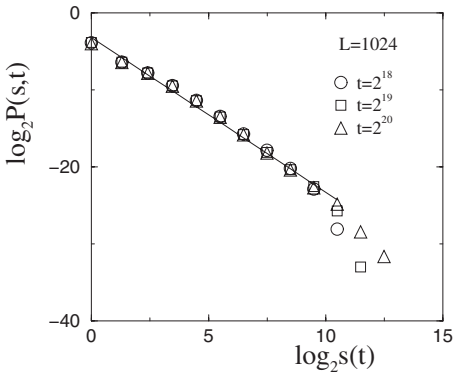

FIG. 11. Plot of cluster size distribution $P(s,t)$ for $L=1024$ at $t=2^{18}$, 2^{19}, and 2^{20}. The straight line represents the least square fitting through the first 11 data points at $t=2^{20}$ and has a slope -2.01 ± 0.06.

$$P(s,t) = N_s(t)/N_{\text{tot}}(t) \sim s(t)^{-\tau}, \tag{13}$$

where $N_s(t)$ is the number of s-sited clusters out of total N_{tot} clusters found at that time, τ is a new exponent. The cluster size distribution $P(s,t)$ is plotted in Fig. 11 for $L=1024$ at $t=2^{18}$, 2^{19}, and 2^{20}. The straight line represents the least square fitting between the first 11 data points of $t=2^{20}$. The slope of the straight line is found as -2.01 ± 0.06. The dynamical cluster size then has a power-law distribution with $\tau\approx2$ as in percolation (187/91) [21]. However, the power-law distribution is obtained here in a nonequilibrium steady state. In case of percolation, the criticality characterized by power-law distribution of cluster size occurs at a equilibrium critical state achieved by tuning the occupation probability p to p_c. On the contrary, the system here tunes itself to the dissolution threshold $r_c(\approx p_c)$ and achieves the nonequilibrium steady state spontaneously. It is thus a SOC [13] state driven by a SEPG in the invasion of a complex solid.

In SOC models, the system is slowly driven externally by adding sand grains [30] whereas a constant source of solution is provided here to maintain the steady state. Beside the scale-free nature of $P(s,t)$ and slow driving, the system has other essential properties such as constant flux, mass conservation, and diffusive growth of a SOC systems [31]. An avalanche here is a temporal consecutive sequence of dissolution events as in IP [17]. However, the growth of an avalanche could be interrupted here by redeposition in contrast to IP which also lacks mass conservation.

IX. SUMMARY

In summary, invasion of a sticky random solid by a constant source of solution is modeled via a chemical reaction of dissolution and reconstruction of the interface. A self-established potential gradient in the binding energy is developed spontaneously and separates the solid into restructured "hard solid" from the original "soft solid." The solution molecules form clusters and are drifted together as a Gaussian profile inside the solid at a constant speed. The system organizes itself to a nonequilibrium steady state. In the steady state, the system is found consisting of finite clusters of solution molecules followed by a path of redeposited solid as an invasion percolation cluster. The growth of the interface as well as the cluster size is found diffusive with time. The cluster size has a power-law distribution characterizing the steady state as critical corresponding to p_c. A self-organized critical behavior at a nonequilibrium steady state driven by a self-established potential gradient in a random system is then observed. The present model has connections with systems defined in multidisciplinary topics of statistical physics such as invasion percolation, glass dissolution, SOC, reaction diffusion, driven interface in disordered media, biological evolution, particles on evolving surfaces, etc.

ACKNOWLEDGMENTS

The authors thank Deepak Dhar for helpful discussions. Financial assistance from BRNS, DAE, Government of India is gratefully acknowledged.

[1] M. Sahimi, *Flow and Transport in Porous Media and Fractured Rock* (VCH, Weinham, 1995).
[2] M. Rost, L. Laurson, M. Dubé, and M. Alava, Phys. Rev. Lett. **98**, 054502 (2007).
[3] K. J. Måløy, S. Santucci, J. Schmittbuhl, and R. Toussaint, Phys. Rev. Lett. **96**, 045501 (2006).
[4] R. Albert, A. L. Barabási, N. Carle, and A. Dougherty, Phys. Rev. Lett. **81**, 2926 (1998).
[5] V. Hardy, S. N. Majumdar, M. R. Lees, D. McK. Paul, C. Yaicle, and M. Hervieu, Phys. Rev. B **70**, 104423 (2004).
[6] J. Soriano, A. Mercier, R. Planet, A. Hernández-Machado, M. A. Rodriguez, and J. Ortin, Phys. Rev. Lett. **95**, 104501 (2005).
[7] D. Wilkinson and J. F. Willemsen, J. Phys. A **16**, 3365 (1983).
[8] R. Lenormand and C. Zarcone, Phys. Rev. Lett. **54**, 2226 (1985).
[9] M. M. Dias and D. J. Wilkinson, J. Phys. A **19**, 3131 (1986).
[10] J. Feder, *Fractals* (Plenum, New York, 1989).
[11] M. A. Knackstedt, M. Sahimi, and A. P. Sheppard, Phys. Rev. E **65**, 035101(R) (2002).
[12] R. K. Iler, *The Chemistry of Silica* (Wiley, New York, 1979).
[13] K. Christensen and N. R. Moloney, *Complexity and Criticality* (Imperial College Press, London, 2005).
[14] O. Deruelle, O. Spalla, P. Barboux, and J. Lambard, J. Non-Cryst. Solids **261**, 237 (2000); L. Sicard, O. Spalla, F. Né, O. Taché, and P. Barboux, J. Phys. Chem. C **112**, 1594 (2008).
[15] S. B. Santra, B. Sapoval, P. Barboux, and F. Devreux, C. R. Acad. Sci., Ser. IIb Mec. Phys. Astron. **326**, 129 (1998).
[16] S. Sinha, V. Kishore, and S. B. Santra, Europhys. Lett. **71**, 632 (2005).
[17] A. Gabrielli, G. Caldarelli, and L. Pietronero, Phys. Rev. E **62**, 7638 (2000).
[18] J. E. de Freitas, L. S. Lucena, and S. Roux, Physica A **266**, 81 (1996); Phys. Rev. E **64**, 051405 (2001).

[19] P. Grassberger and Y. C. Zhang, Physica A **224**, 169 (1996).
[20] A. M. Alencar, J. S. Andrade, Jr., and L. S. Lucena, Phys. Rev. E **56**, R2379 (1997).
[21] A. Bunde and S. Havlin, *Fractals and Disordered Systems* (Springer-Verlag, Berlin, 1991).
[22] Z. V. Djordjevic, S. Havlin, H. E. Stanley, and G. H. Weiss, Phys. Rev. B **30**, 478 (1984).
[23] H. J. Herrmann and H. E. Stanley, J. Phys. A **21**, L829 (1988); U. A. Neumann and S. Havlin, J. Stat. Phys. **52**, 203 (1988).
[24] A. Ledieua, F. Devreuxa, and P. Barbouxa, J. Non-Cryst. Solids **345-346**, 715 (2004).
[25] J. Mai, I. M. Sokolov, and A. Blumen, Phys. Rev. Lett. **77**, 4462 (1996).
[26] E. Ben-Jacob, I. Cohen, and H. Levine, Adv. Phys. **49**, 395 (2000).
[27] J. D. Murray, *Mathematical Biology* (Springer-Verlag, New York, 2003).
[28] A. Nagar, M. Barma, and S. N. Majumdar, Phys. Rev. Lett. **94**, 240601 (2005).
[29] P. Bak and K. Sneppen, Phys. Rev. Lett. **71**, 4083 (1993).
[30] S. B. Santra, S. Ranjita Chanu, and D. Deb, Phys. Rev. E **75**, 041122 (2007), and references therein.
[31] S. S. Manna and A. L. Stela, Physica A **316**, 135 (2002).